JOURNAL OF BACTERIOLOGY, Sept. 2004, p. 6220–6229 Vol. 186, No. 18
0021-9193/04/$08.00+0 DOI: 10.1128/JB.186.18.6220–6229.2004

The hFbpABC Transporter from *Haemophilus influenzae* Functions as a Binding-Protein-Dependent ABC Transporter with High Specificity and Affinity for Ferric Iron

Damon S. Anderson,[1] Pratima Adhikari,[1] Andrew J. Nowalk,[2] Cheng Y. Chen,[3] and Timothy A. Mietzner[1]*

Department of Molecular Genetics and Biochemistry[1] and Department of Pediatrics,[2] University of Pittsburgh School of Medicine, Pittsburgh, Pennsylvania, and Sexually Transmitted Diseases and Tuberculosis Laboratory Research, Division of AIDS, National Center for Infectious Diseases, Centers for Disease Control and Prevention, Atlanta, Georgia[3]

Received 4 June 2004/Accepted 9 June 2004

Pathogenic *Haemophilus influenzae*, *Neisseria* spp. (*Neisseria gonorrhoeae* and *N. meningitidis*), *Serratia marcescens*, and other gram-negative bacteria utilize a periplasm-to-cytosol FbpABC iron transporter. In this study, we investigated the *H. influenzae* FbpABC transporter in a siderophore-deficient *Escherichia coli* background to assess biochemical aspects of FbpABC transporter function. Using a radiolabeled Fe^{3+} transport assay, we established an apparent K_m = 0.9 μM and V_{max} = 1.8 pmol/10^7cells/min for FbpABC-mediated transport. Complementation experiments showed that hFbpABC is dependent on the FbpA binding protein for transport. The ATPase inhibitor sodium orthovanadate demonstrated dose-dependent inhibition of FbpABC transport, while the protonmotive-force-inhibitor carbonyl cyanide *m*-chlorophenyl hydrazone had no effect. Metal competition experiments demonstrated that the transporter has high specificity for Fe^{3+} and selectivity for trivalent metals, including Ga^{3+} and Al^{3+}, over divalent metals. Metal sensitivity experiments showed that several divalent metals, including copper, nickel, and zinc, exhibited general toxicity towards *E. coli*. Significantly, gallium-induced toxicity was specific only to *E. coli* expressing FbpABC. A single-amino-acid mutation in the gene encoding the periplasmic binding protein, FbpA(Y196I), resulted in a greatly diminished iron binding affinity $K_d = 5.2 \times 10^{-4}$ M^{-1}, ~14 orders of magnitude weaker than that of the wild-type protein. Surprisingly, the mutant transporter [FbpA(Y196I)BC] exhibited substantial transport activity, ~35% of wild-type transport, with K_m = 1.2 μM and V_{max} = 0.5 pmol/10^7cells/min. We conclude that the FbpABC complexes possess basic characteristics representative of the family of bacterial binding protein-dependent ABC transporters. However, the specificity and high-affinity binding characteristics suggest that the FbpABC transporters function as specialized transporters satisfying the strict chemical requirements of ferric iron (Fe^{3+}) binding and membrane transport.

To cause disease, many bacterial pathogens must compete for growth-essential iron within the extracellular environment of the human host (30, 33, 45). The majority of pathogenic bacteria employ siderophore-dependent iron acquisition systems in competition for host iron (47). These systems involve the use of nonproteinaceous iron-chelating compounds termed siderophores, which are produced and secreted into the environment (32). In gram-negative bacteria the uptake of iron-bound siderophores involves the expression of siderophore-specific outer membrane receptors and specific inner membrane binding protein-dependent ATP-binding cassette (ABC) transporters (14). These systems offer flexibility in the acquisition of iron from multiple sources; however, the expression of the numerous gene products involved in each specific siderophore-dependent transport pathway may be metabolically demanding.

In contrast, *Haemophilus influenzae* and pathogenic *Neisseria* spp. (*Neisseria meningitidis* and *N. gonorrhoeae*) utilize a highly conserved siderophore-independent high-affinity iron acquisition system (31). This system employs specific surface receptors that directly bind host iron-binding proteins, transferrin (Tf) or lactoferrin (Lf) (37). Iron is extracted from the host proteins and transported into the periplasm through an energy-dependent TonB-mediated process. Transport of free (naked) iron from the periplasm to the cytosol is mediated via the FbpABC transporter, which is composed of a ferric ion binding protein (FbpA) and an inner membrane ABC transporter consisting of a membrane permease (FbpB) and an ATP-binding protein (FbpC) (1). Although bacteria utilizing this system may express several different host protein-specific outer membrane receptors, FbpABC is a convergence point in the acquisition of iron.

By a strategy similar to that used in cloning the *Serratia marcescens sfuABC* operon (5), the *H. influenzae hitABC* and *N. gonorrhoeae fbpABC* operons were cloned by complementation of a siderophore-deficient (*aroB*) *Escherichia coli* strain for growth on nutrient agar containing 200 μM dipyridyl, an iron chelator (1, 2). Expression in this *E. coli* background has served as a model system with which to study the genetic and biochemical basis of FbpABC iron transport. Results of initial studies demonstrated that the transporter genes from these diverse bacteria exhibit a high level of homology, and a common nomenclature has been devised to designate the genetic

* Corresponding author. Mailing address: Department of Molecular Genetics and Biochemistry, University of Pittsburgh School of Medicine, Room E1240 Biomedical Science Tower, Lothrop St., Pittsburgh, PA 15261. Phone: (412) 648-9244. Fax: (412) 624-1401. E-mail: mietzner@pitt.edu.

and protein components of the transporters: for *H. influenzae*, the gene name is *hitABC* and the protein name is hFbpABC; for *N. gonorrhoeae*, the gene name is *fbpABC* and the protein name is nFbpABC. The FbpABC transporters are encoded by three-gene operons under negative regulatory control of the ferric uptake regulator (*fur*) (7, 15). The gene encoding the ferric ion binding protein (FbpA) is separated from the downstream two genes in the operon by a putative stem loop structure indicative of a rho-independent transcriptional terminator. This is consistent with the increase in expression of FbpA by several orders of magnitude compared with that of FbpB and FbpC (26). Biochemical analyses of nFbpA and hFbpA demonstrate that these proteins bind a single ferric (Fe^{3+}) ion with high affinity and exhibit a characteristic spectroscopic profile (13, 34, 35). Interestingly, X-ray structural analyses of these proteins show that they bind iron in a manner remarkably similar to that of mammalian transferrin by using a common set of amino acid residues and employing a synergistic anion (10, 11). This FbpA binding mechanism results in an extremely high affinity for Fe^{3+}, similar in scale to that of Tf (nFbpA, $2.4 \times 10^{18}\ M^{-1}$; N-lobe hTf, $1.8 \times 10^{17}\ M^{-1}$) (44, 49). However, this affinity is 10 to 12 orders of magnitude greater than the affinities exhibited by typical bacterial periplasmic binding proteins (PBPs) for their respective substrates (e.g., maltose binding protein for maltose; $K_d = 1.6 \times 10^{-6}$ M) (18). Based on sequence analysis, the nFbpB and hFbpB proteins are proposed highly hydrophobic proteins that function as membrane permeases within the context of the ABC transporters. The nFbpC and hFbpC proteins are proposed ATP-binding components of these transporters (31). The large number of recent studies on the FbpA ferric binding proteins (3, 8, 10, 16, 19, 22, 38–40, 44, 50) makes a critical investigation of the functional basis of FbpABC transport timely.

This study focuses on functional investigation of the *H. influenzae* hFbpABC transporter through expression of the *hitABC* three-gene locus in *E. coli*. Recombinant expression in this background includes the use of an *E. coli* strain (H-1443) that has a deletion in the *aroB* gene, rendering it unable to synthesize the sole *E. coli* siderophore enterochelin (9). This background allows investigation of the hFbpABC system while controlling for endogenous iron uptake systems (e.g., *FepABCD*, *FecABCDE*, *FeoABC*, and *MntH*) (17, 25, 28, 41) by the use of high-affinity metal chelators, 2,2,-dipyridyl, and nitrilotriacetic acid. Using this model system, we established an assay for radiolabeled iron uptake in intact cells and generated apparent Michaelis-Menten K_m and V_{max} constants for hFbpABC transport. We then defined the energy requirements and metal specificity of hFbpABC by monitoring the growth-inhibitory effects of metals competing for hFbpABC-mediated transport. Finally, we investigated the impact of a single-amino-acid hFbpA mutation on hFbpABC-mediated transport and derived the functional basis of this effect. These studies form the basis of continuing investigations aimed at augmenting our understanding of FbpABC iron transport and its contribution to pathogenesis of diverse bacterial species.

MATERIALS AND METHODS

Biochemicals, plasmids, and bacterial strains. Ampicillin, L-arabinose, 2,2′-dipyridyl, MES (morpholineethanesulfonic acid) and Tris buffers, glucose, carbonyl cyanide *m*-chlorophenyl hydrazone (CCCP), nitrilotriacetic acid (NTA), cetyltrimethylammonium bromide (CTAB), cupric chloride, aluminum sulfate, zinc chloride, manganese sulfate, nickelous chloride, phenylalanine, tyrosine, tryptophan, and sodium orthovanadate were purchased from Sigma (St. Louis, Mo.). Nutrient broth (NB), Luria broth (LB), Bacto agar, and sterile supplement disks were purchased from Difco Laboratories (Detroit, Mich.). Chelex-100 and sodium dodecyl sulfate-polyacrylamide gel electrophoresis reagents were purchased from Bio-Rad (Hercules, Calif.). Ferric nitrate and gallium nitrate were purchased from Aldrich (Milwaukee, Wis.). ^{55}Ferric chloride was purchased from NEN (Boston, Mass.). ^{67}Gallium citrate was a generous gift from Robert Schork of University of Pittsburgh Medical Center Presbyterian Nuclear Medicine. Oligonucleotides were purchased from Gibco/Life Technologies (Gaithersburg, Md.). *Taq* polymerase was purchased from Boehringer Mannheim (Mannheim, Germany). Restriction enzymes were purchased from New England Biolabs (Beverly, Mass.). Nitrocellulose filters and scintillation cocktail were obtained from Fisher (Pittsburgh, Pa.). *E. coli* strains and plasmids were obtained as described in Table 1.

Molecular cloning. The pAHIΔB plasmid was constructed by excision of the *hitB* gene from the MluI sites of the pAHIO plasmid. The resulting MluI-compatible ends were ligated, and the coding sequence was verified by automated DNA sequencing (Department of Molecular Genetics and Biochemistry Shared Resources Facility, University of Pittsburgh). The pACYCHIΔB and pACYCHIO plasmids were made by PCR amplification of the *hitABC* genes and ~250 kb of upstream and downstream sequence from the pAHIO plasmid by the use of the HitO-5′ and HitO-3′ primers described previously (2). The PCR product was restricted with BamHI and SmaI and ligated into compatible BamHI and EcoRV sites of the pACYC184 vector. The pBADHIBC plasmid was constructed by PCR amplification of the *hitBC* genes from the pAHIO plasmid by the use of the primers HitB5′TA (5′-ATGCCTCGCAGACCGCCA TTCTGGCTTAC-3′) and HitC3′TA (5′-AGCGTAAAAAAGCCCTTTTTT ATGTAAATA-3′). pBAD-TOPO-TA vector (Invitrogen, Carlsbad, Calif.) was used in direct TA cloning of the PCR product.

Iron transport assay. NB agar (NBA) and LB agar (LBA) were prepared per manufacturer instructions and supplemented with ampicillin and/or dipyridyl. M9 minimal medium (M9) was prepared, with the following final composition: 6 mg of Na_2HPO_4/ml, 3 mg of KH_2PO4/ml, 0.5 mg of NaCl/ml, 1 mg of NH_4Cl/ml, 5 mM $MgSO_4$, and 0.1 mM $CaCl_2$. Prior to sterilization, trace iron was removed from M9 by stirring in the presence of 100 mg of Chelex-100/liter followed by sterile filtration. Transport medium (TM) was prepared by supplementing M9 with 2 mg of glucose/ml, 0.1 mg of phenylalanine/ml, 0.1 mg of tyrosine/ml, and 0.1 mg of tryptophan/ml; radiolabeled $Fe(NTA)_2$ or $Ga(NTA)_2$ was added immediately prior to the assay. Cells were transformed using the heat shock method for chemically competent cells. Fresh transformants were grown to midlog phase in LB supplemented with 100 μg of ampicillin/ml ($LBamp_{100}$), seeded at 10^6 CFU/plate on NBA supplemented with 100 μg of ampicillin/ml and 75 μM dipyridyl ($NBAamp_{100}dip_{75}$), and then grown at 37°C for 18 h. Cells were suspended in M9 and centrifuged at 4°C for 10 min at 4,000 × *g*. Pelleted cells were brought up in TM and diluted to an optical density at 578 nm of 0.5. The cells were then preincubated at 37°C in 5% CO_2 with shaking in 24-well tissue culture plates in a water-jacketed incubator. Following a 10-min preincubation, radiolabeled $Fe(NTA)_2$ (3×10^4 cpm/pmol) was added to the cell suspensions at a final concentration of 1 μM and incubation was continued. At designated time points, 100-μl aliquots were removed and filtered through 0.45-μm-pore-size nitrocellulose filters (filters conditioned with 5 ml of TM) by the use of a vacuum manifold (Millipore, Billerica, Mass.). Filters were immediately washed with 5 ml of 100 mM LiCl, removed, and air dried overnight at 25°C. The filters were dissolved in 4 ml of scintillation cocktail, and counts per minute were measured using a liquid scintillation counter (Packard, Billerica, Mass.).

In complementation experiments, cells were grown as described above except that the growth medium contained 30 μg of chloramphenicol/ml for pACYC vector selection and 0.2% L-arabinose to induce expression of *hitBC* under the control of the *ara*BAD (pBAD) promoter.

Kinetics of iron transport. Michaelis-Menten constants for the wild-type hFbpABC and mutant hFbpA(Y196I)BC transporters were determined using the above-described iron transport assay with the following conditions. Cells were used at a concentration of 10^7 cells per 100 μl, and substrate concentrations were adjusted over a range of 0.1 to 20 μM. Initial velocity measurements were determined by taking 100-μl samples at 5 and 120 s and determining counts per minute for the difference (115-s uptake). Substrate-dependent uptake was determined by subtracting hFbpA-only background uptake (with pAHIΔB or pAHIΔBAY196I) from hFbpABC uptake (with pAHIO or pAHIOAY196I) and plotting initial velocity (in picomoles/10^7 cells/minute) against substrate concentration (in micromoles). Results were not significantly affected by the use of higher cell concentrations (10^7 to 10^9 cells/100 μl). Data were from a single experiment and

TABLE 1. Bacterial Strains and Plasmids

Strain or plasmid	Characteristics	Reference or source
Strains		
H-1443	*E. coli* aroB$^-$	9
H-1443/pBR322	H-1443 with pBR322	This study
H-1443/pAHIΔB	H-1443 with *hitA, hitC*	This study
H-1443/pAHIO	H-1443 with *hitABC*	2
H-1443/pAHIΔBAY196I	H-1443 with *hitA(Y1961), hitC*	This study
H-1443/pAHIOAY196I	H-1443 with *hitA(Y1961)BC*	This study
H-1443/pACYC184-pBADHIBC	H-1443 with pACYC184 and *hitBC*	This study
H-1443/pACYCHIΔB-pBADHIBC	H-1443 with *hitA*, *hitC*, and *hitBC*	This study
H-1443/pACYCHIO-pBADHIBC	H-1443 with *hitABC* and *hitBC*	This study
Plasmids		
pBR322	4.4-kb vector, Ap^r	Promega
pAHIO	4.3-kb SmaI-BamHI fragment containing intact *hitABC* sequence cloned into corresponding sites in pBR322, expressing hFbpABC, Ap^r	2
pAHIΔB	pAHIO derivative, lacking *hitB* gene, expressing functional hFbpA, Ap^r	This study
pAHIOAY196I	Site-directed mutant derived from pAHIO, expressing hFbpA(Y196I)BC, Ap^r	This study
pAHIΔBAY196I	pAHIOAY196I derivative lacking *hitB* gene, expressing functional hFbpA(Y196I), Ap^r	This study
pACYC184	4.25-kb vector, Cm^r, Tc^r	New England Biolabs
pACYCHIO	4.3-kb SmaI-BamHI fragment containing intact *hitABC* sequence cloned into EcoRV-BamHI sites in pACYC184, expressing hFbpABC, Cm^r	This study
pACYCHIΔB	pACYCHIO derivative lacking *hitB* gene, expressing hFbpA, Cm^r	This study
pBADHIBC	2.6-kb fragment containing *hitBC* sequence cloned into pBADtopoTA (Invitrogen), expressing hFbpBC Ap^r	This study

are representative of data obtained from at least three replicate assays. Nonlinear regression analysis was performed using Origin 7 graphing software.

Complementation studies. H-1443/pACYC184-pBADHIBC, H-1443/pACYCHIΔB-pBADHIBC, and H-1443/pACYCHIO-pBADHIBC were grown in $LBamp_{100}cam_{30}$ to midlog phase. Cells were seeded at 10^6 CFU/plate on $NBAamp_{100}cam_{30}dip_{75}$ supplemented with 0.2% arabinose and incubated at 37°C for 24 h. The radiolabeled $Fe(NTA)_2$ transport assay was performed as described above.

Energy utilization, metal competition, and metal sensitivity of hFbpABC. The metabolic inhibitor CCCP or sodium orthovanadate was added 1 or 10 min prior to the addition of radiolabeled $Fe(NTA)_2$, respectively. In metal competition experiments, $metal(NTA)_2$ complexes were added 1 min prior to addition of labeled $Fe(NTA)_2$. Metal sensitivity experiments were performed by growing fresh transformants of H-1443/pBR322, H-1443/pAHIΔB, and H-1443/pAHIO in $LBamp_{100}$ to midlog phase, diluting, and seeding on $NBAamp_{100}$ at 10^4 CFU/plate. Upon drying, sterile disks were placed on the plates to which the following metal salts (200 mM) were applied: $NiCl_2$, $MnSO_4$, $ZnCl_2$, $AlSO_4$, $CuCl_2$, and $Ga(NO_3)_3$. The plates were inverted and incubated at 37°C for 18 h. Following incubation the plates were digitally scanned.

Gallium transport assay. The radiolabeled $Ga(NTA)_2$ transport assay was performed under conditions similar to those for the iron transport assay, using $^{67}Ga(NTA)_2$ at 3×10^4 cpm/pmol. Dried nitrocellulose filters were subjected to direct counting using a gamma counter (Packard).

Construction and purification of the hFbpA(Y196I) mutant. Selection of the Tyr196Ile mutation was performed on the basis of the crystal structures of hFbpA and a homologous nFbpA mutant (35). The mutant was constructed using a Gene Editor system (Promega, Madison, Wis.), with the pAHIO plasmid as the template. The mutation was verified by DNA sequencing as described above. The hFbpA(Y196I) protein was purified using a modification of a previously reported protocol (2). Briefly, an overnight culture of JM109/pAHIOAY196I was used to inoculate 1 liter of $NBamp_{100}$ and the culture was grown at 37°C with shaking for 18 h. Cells were harvested by centrifugation ($4,000 \times g$, 15 min) and washed in phosphate-buffered saline. The cells were then resuspended in a 50-ml solution of 400 mM Tris (pH 8.0)–2% (wt/vol) CTAB and shaken at 37°C for 2 h. Cell debris was removed by centrifugation, and the soluble lysate was diluted to 500 ml in water. The diluted lysate was clarified by filtration and applied to a carboxymethyl-Sepharose CL-6B column equilibrated with 10 mM Tris (pH 7.5). The column was washed with 10 volumes of 10 mM Tris (pH 7.5) and subjected to several step washes: 4 volumes of 10 mM Tris (pH 7.5)–200 mM NaCl, 4 volumes of 400 mM NaCl, and 4 volumes of 500 mM NaCl. Purified hFbpA(Y196I) was collected following a gradient elution of 500 to 1,000 mM NaCl. Fractions were analyzed for protein content by monitoring the A_{280} and assessed for purity using sodium dodecyl sulfate-polyacrylamide gel electrophoresis. hFbpA(Y196I)-containing fractions were pooled and concentrated in an Amicon concentration cell with a 10-kDa-cutoff Diaflo ultrafiltration membrane and then dialyzed using 20 mM MES (pH 6.5)–200 mM NaCl. Wild-type hFbpA was purified according to a previously published protocol (2). Iron was removed from the hFbpA proteins by incubation with 1,000-fold-molar-excess sodium citrate (pH 6.0) on ice for 30 min. Protein was then dialyzed using 10 volumes of 10 mM sodium citrate followed by exhaustive dialysis using iron-free 20 mM MES (pH 6.5)–200 mM NaCl. Concentrated protein was kept at −80°C.

UV/Vis spectroscopy of hFbpA and hFbpA(Y196I). The visible absorbances of iron-saturated hFbpA and hFbpA(Y196I) were measured using 30 μM solutions of protein in 20 mM MES (pH 6.5)–200 mM NaCl. Protein was incubated with $Fe(NTA)_2$ (1.2 molar equivalents) for 2 days at 4°C. Absorbance spectra were acquired using an AVIV model 14 UV/Vis spectrophotometer. Three scans of each protein were taken, and the results were averaged. Data were plotted using Cricket Graph III.

Iron binding affinity of hFbpA(Y196I). The effective Fe^{3+} dissociation constant (K_d) of hFbpA(Y196I) was determined using equilibrium binding and ultrafiltration methods. Iron-free hFbpA(Y196I) (15 μM) in 20 mM MES (pH 6.5)–100 mM NaCl–150 μM $NaPO_4$ was incubated in the presence of increasing concentrations of $Fe(NTA)_2$ labeled with $^{55}FeCl_3$ (7×10^4 cpm/μl) for 2 days at 4°C. The solutions were subjected to filtration using BIOMAX ultrafree filter tubes with 10 NMWL membranes centrifuged at $10,000 \times g$ for 5 min at 4°C. Aliquots of both the total protein solution [bound plus free $Fe(NTA)_2$] and the filtrate [free $Fe(NTA)_2$] were removed and measured for radioactivity by the use of a liquid scintillation counter. Bound iron (total minus filtrate) was plotted versus the total iron concentration, and nonlinear regression analysis was performed using Origin 7 graphing software.

RESULTS

hFbpABC iron transport. Previous work demonstrated that propagation on NBA supplemented with 200 μM dipyridyl allows the selection of H-1443 *E. coli* complemented with a

functional *hitABC* operon (2). In this study, $NBAamp_{100}$ supplemented with 75 μM dip ($NBAamp_{100}dip_{75}$) allowed growth of H-1443 *E. coli* while forcing upregulation of *hitABC* derived from the pAHIO plasmid, which is under the transcriptional control of the *H. influenzae fur* operator. Growth on $NBAamp_{100}dip_{75}$ medium followed by suspension in iron-free M9 was found to be the optimal condition for measuring iron transport. In this transport assay, $^{55}Fe^{3+}$ was provided as a nitrilotriacetate complex for several reasons: (i) previous work has demonstrated that $Fe(NTA)_2$ is very efficient in loading FbpA with Fe^{3+}, as NTA can serve as the synergistic anion (16); (ii) once bound, the NTA anion readily exchanges with other endogenous anions, including PO_4, the preferred anion (16); and (iii) the affinity of NTA for Fe^{3+} is sufficiently high to inhibit competition by *E. coli* low-affinity iron transport systems. H-1443 *E. coli* was transformed with pBR322, pAHIΔB, or pAHIO plasmid (pAHIO and mutants used in this study were derived from the pBR322 background and thus have identical copy numbers). Fresh transformants were grown on $NBAamp_{100}dip_{75}$, washed with M9, and measured via the transport assay (Fig. 1).

In this assay, H-1443/pBR322 demonstrated minimal iron uptake (~0.38 pmol $Fe/10^9$ cells at time = 6 min [2.1% of pAHIO results]), indicating negligible effects of the *E. coli* strain under assay conditions with $Fe(NTA)_2$ as a supplement (Fig. 1A). The H-1443/pAHIΔB control demonstrated a low-level time-dependent increase in signal (~4.29 pmol $Fe/10^9$ cells at time = 6 min [23.3% of pAHIO results]) compared to the background (H-1443/pBR322) (Fig. 1A). The signal result is not due to functional iron transport via hFbpABC but rather is due to binding of labeled $Fe(NTA)_2$ to hFbpA within the periplasm of these cells. This is consistent with previous results that showed that pAHIΔC was unable to mobilize iron into the cytosol of H-1443 *E. coli* (2). Subsequently, the activities of both pAHIΔB and pAHIΔC were measured using the transport assay and shown to be very similar (data not shown). The pAHIΔB control was used in the present study to eliminate any interference the presence of the hFbpB permease may exert on transport analyses. Levels of hFbpA expression by both pAHIΔB and pAHIO were measured by Western blot and densitometric analysis (Kodak Imagestation 1000) and found to be identical (pAHIΔB:pAHIO, 1.0:0.942), indicating that the difference in signal results between pAHIΔB and pAHIO (see below) was not the result of altered levels of hFbpA expression (Fig. 1B).

To address the observation that pAHIΔB does not reach time-dependent saturation, H-1443/pAHIΔB cells were subjected to chasing with 100-fold-excess unlabeled $Fe(NTA)_2$ at the 6-min time point (Fig. 1A). The chase resulted in a >50% loss of signal, indicating release of $Fe(NTA)_2$ from hFbpA within the periplasm of the cells. The nonsaturable pAHIΔB signal may be due to the possibility that hFbpA within the H-1443/pAHIΔB periplasm is nearly saturated with unlabeled iron from the growth medium (the concentration of Fe^{3+} in NBA is approximately 10 μM [personal observation]). Thus, the rate of binding for 1 μM $^{55}Fe(NTA)_2$ to hFbpA is likely slow and would require increased time to reach saturation.

The H-1443/pAHIΔB control served as a baseline in the measurement of functional hFbpABC-mediated transport. The full transporter H-1443/pAHIO demonstrated a high-level time-dependent increase in signal (~18.37 pmol $Fe/10^9$ cells at time = 6 min) (Fig. 1A). These results demonstrate that the assay is a specific measure of hFbpABC transport and is of sufficient sensitivity to test multiple parameters of hFbpABC transporter function, including metal specificity, energy requirements, and the effects of mutations.

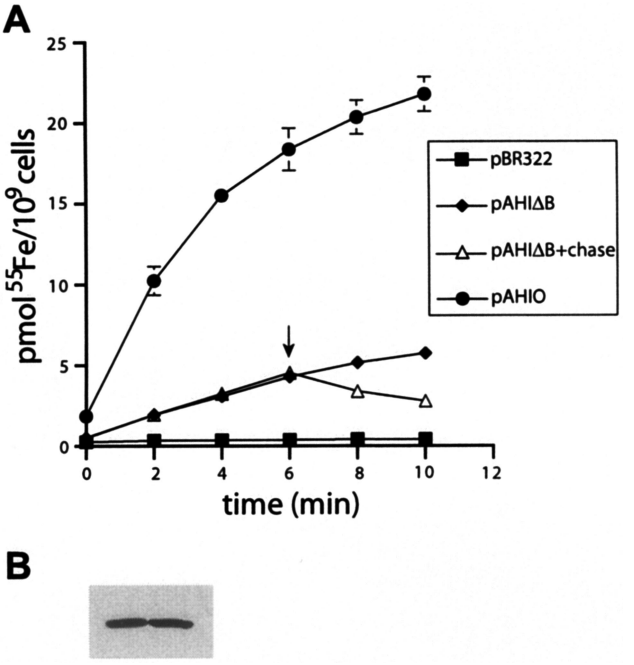

FIG. 1. hFbpABC $^{55}Fe^{3+}$ transport assay. (A) Cells grown on $NBAamp_{100}dip_{75}$ were resuspended in TM, preincubated for 10 min at 37°C, and supplemented with 1 μM $^{55}Fe(NTA)_2$. Samples were taken at 2-min intervals and subjected to filtration, and counts per minute were determined. Radiolabeled iron uptake is plotted versus time. Each strain was tested in triplicate; error bars represent standard deviations (SD). pAHIΔB+chase, pAHIΔB in which 100-fold-excess unlabeled $Fe(NTA)_2$ was added at 6 min (arrow). (B) Western blot of lysates from pAHIΔB (left lane) and pAHIO (right lane) probed with anti-hFbpA-specific antibody. Densitometric analysis demonstrated similar levels of hFbpA expression in these cultures (pAHIΔB:pAHIO, 1.0:0.942).

Kinetics of hFbpABC transport. Incubation of pAHIO/H-1443 with increasing concentrations of $^{55}Fe(NTA)_2$ demonstrated saturation of transport characteristic of Michaelis-Menten kinetics. After subtracting the pAHIΔB control results, the pAHIO transport rates were used to calculate estimated values for K_m and V_{max}. The estimated apparent K_m for wild-type hFbpABC Fe^{3+} transport was 0.9 μM, and the apparent V_{max} was 1.8 pmol/10^7cells/min. These values are within a close range of those derived for other binding protein-dependent ABC transport systems, including the maltose and histidine transporters (4, 29), and demonstrate that the hFbpABC transporter functions with a substrate turnover similar to those of other bacterial small-ligand transporters.

hFbpABC is a binding protein-dependent ABC transporter. To demonstrate that the hFbpABC transporter is dependent upon the binding protein for function, complementation experiments were performed. Initially, the qualitative assay of growth or absence of growth on $NBAamp_{100}cam_{30}$ containing 200 μM dipyridyl was used to determine whether hFbpA

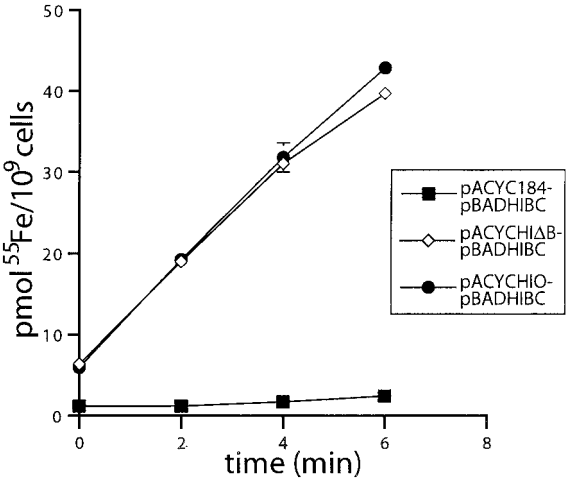

FIG. 2. hFbpABC is a binding protein-dependent ABC transporter. *E. coli* H-1443 cells expressing the hFbpBC proteins only (pACYC184-pBADHIBC) demonstrated minimal Fe^{3+} uptake similar in scale to vector-only cells (Fig. 1A). Cells expressing the hFbpBC proteins complemented with hFbpA (pACYCHIΔB-pBADHIBC) demonstrated a high level of Fe^{3+} uptake similar in scale to cells expressing the full hFbpABC transporter (pACYCHIO-pBADHIBC). Thus, the ABC transporter (hFbpBC) functions in iron transport only in the presence of the binding protein (hFbpA).

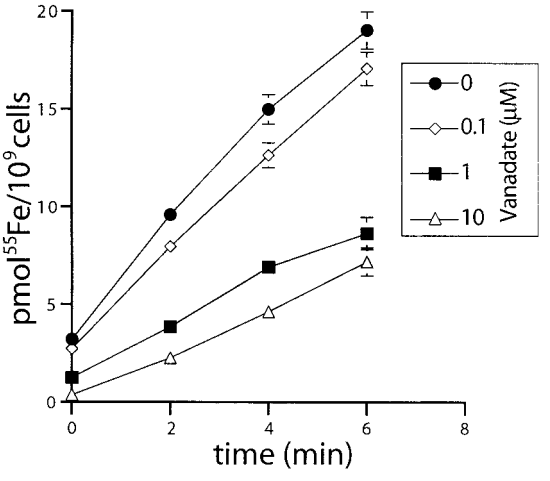

FIG. 3. Energy requirements of hFbpABC. The ATPase inhibitor sodium orthovanadate (0.1, 1, or 10 mM) was added 10 min prior to $^{55}Fe(NTA)_2$. Samples were collected and measured as described in Materials and Methods. Each strain was tested in triplicate; error bars represent SD. The protonophore CCCP (50 or 250 μM) was added 1 min prior to $^{55}Fe(NTA)_2$, with minimal effects on transport (data not shown).

could complement hFbpBC expressed under the control of an exogenous promoter (P_{BAD}) (data not shown). Results showed that H-1443 cells expressing the hFbpBC proteins only (pACYC184-pBADHIBC) exhibited no growth on $NBAamp_{100}cam_{30}dip_{200}$ and that cells expressing hFbpBC complemented with hFbpA (pACYCHIΔB-pBADHIBC) exhibited growth on this medium similar to control cells (pACYCHIO-pBADHIBC). The $^{55}Fe(NTA)_2$ transport assay was used as a more sensitive quantitative measure of complementation. Results demonstrated that the hFbpBC-only cells exhibited a low level of transport similar to background *E. coli* H-1443 cells observed previously (Fig. 1A and 2). Cells expressing hFbpBC complemented with hFbpA (pACYCHIΔB-pBADHIBC) exhibited a high level of $^{55}Fe(NTA)_2$ uptake similar in scale to cells expressing the full hFbpABC transporter (Fig. 2). These results verify that the ABC transporter (hFbpBC) is dependent upon the hFbpA binding protein for functional iron transport.

Energy utilization by hFbpABC. Pretreatment of cells with increasing concentrations of the ATPase inhibitor sodium orthovanadate prior to the addition of $^{55}Fe(NTA)_2$ resulted in a dose-dependent decrease in iron uptake (Fig. 3). This inhibition leveled off at an amount of signal similar to that seen with pAHIΔB, which is indicative of $^{55}Fe(NTA)_2$ binding by hFbpA within the periplasm and loss of cytosolic transport (compare Fig. 3 [10 mM vanadate] with Fig. 1A [pAHIΔB]). These results are consistent with hFbpABC functioning as an ATPase-driven transporter, similar to members of the family of bacterial binding protein-dependent ABC transporters. Interestingly, administration of sodium arsenate under similar conditions had notable effects on transport only at high concentrations (data not shown). This result is likely due to the fact that arsenate has previously been shown to function as a suitable ternary anion in FbpA Fe^{3+} binding. Thus, the presence of arsenate may have the side effect of facilitating hFbpA Fe^{3+} loading and thereby facilitating Fe^{3+} transport. Addition of the protonophore CCCP prior to $^{55}Fe(NTA)_2$ resulted in no apparent effect on iron uptake (data not shown). This is in contrast to the MntH metal permease, which functions as a protonmotive-force-driven symporter and is inhibited by CCCP under similar conditions (28). These results indicate that hFbpABC transport is not driven by protonmotive force.

Metal specificity of hFbpABC. hFbpABC metal specificity was investigated by testing for competition by using trivalent and divalent metals for radiolabeled $Fe(NTA)_2$ transport (Fig. 4). Metal:NTA complexes were added at a 100-fold molar excess to cells 1 min prior to the addition of labeled $Fe(NTA)_2$. Uptake was quenched at the 6-min time point with 100-fold-excess unlabeled $Fe(NTA)_2$. As a control, H-1443/pAHIO to which no competitor was added prior to $^{55}Fe(NTA)_2$ demonstrated a high-level time-dependent increase in iron uptake similar to that shown in Fig. 1A. The competing metals were grouped into one of four categories, minimal, low, medium, and high, on the basis of their abilities to inhibit Fe^{3+} uptake. The divalent metals $Ni(NTA)_2$ and $Zn(NTA)_2$ demonstrated minimal transport competition (13.8 and 22% inhibition of $^{55}Fe^{3+}$ uptake, respectively), while $Cu(NTA)_2$ and $Mn(NTA)_2$ demonstrated low levels of transport competition (34.5 and 36.8% inhibition) (Fig. 4A and B). The trivalent metals $Al(NTA)_2$ and $Ga(NTA)_2$ demonstrated medium competition (48.1 and 53.7% inhibition) (Fig. 4C). None of the metals, however, exhibited high-level competition on a scale similar to $Fe(NTA)_2$ (94.5% inhibition) (Fig. 4D). Taken together, these results demonstrate that the hFbpABC transporter exhibits high specificity for ferric iron and has general selectivity for trivalent metals, including gallium and aluminum, over divalent metals such as copper, manganese, nickel, and zinc.

Metal sensitivity of hFbpABC expressed in H-1443 *E. coli*. Through the course of these studies, several metals tested for metal specificity of hFbpABC (Fig. 4) were identified as inhib-

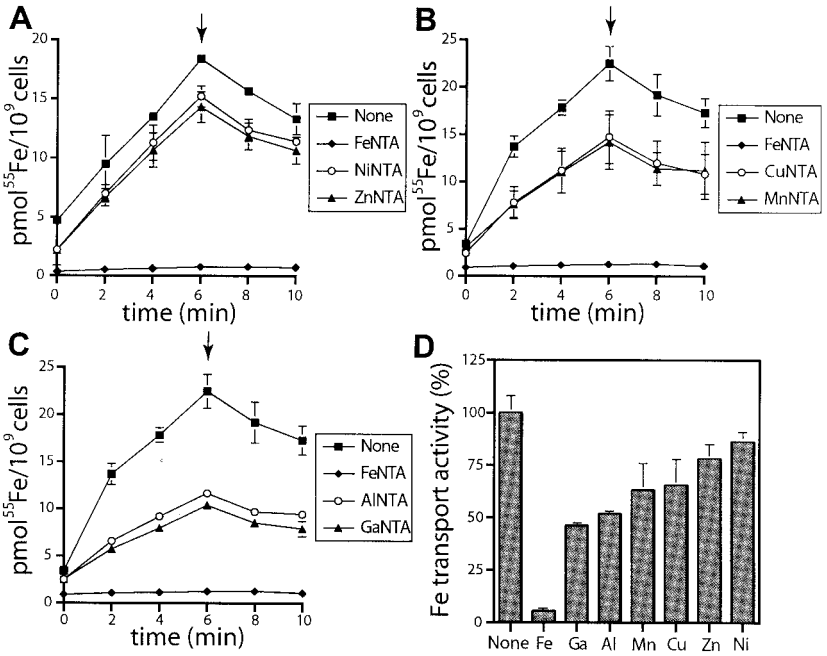

FIG. 4. Metal specificity of hFbpABC. Competing metals [100-fold excess over labeled $^{55}Fe(NTA)_2$] were added 1 min prior to labeled $^{55}Fe(NTA)_2$. Samples were collected and measured as described in Materials and Methods. The arrows indicate quenching of uptake through the addition of 100-fold-excess unlabeled $Fe(NTA)_2$. Each strain was tested in triplicate; error bars represent SD. (A) NiNTA and ZnNTA, (B) CuNTA and MnNTA, (D) AlNTA and GaNTA. (D) Inhibition of hFbpABC-mediated Fe transport. Values at the 6-min time points are compared with that for pAHIO with no competitor (None), and percentages of Fe^{3+} uptake are plotted.

iting the growth of H-1443 *E. coli* expressing hFbpABC. To assess whether hFbpABC was responsible for the toxicity of these metals, the growth-inhibitory effects of specific metals were tested. The results indicate that the divalent metals Cu^{2+}, Ni^{2+}, and Zn^{2+} indeed demonstrate general toxicity to H-1443/pBR322, H-1443/pAHIΔB, and H-1443/pAHIO, independent of hFbpABC (data not shown). Interestingly, Ga^{3+} demonstrated significant toxicity toward H-1443/pAHIO only, indicating a possible correlation between hFbpABC-specific transport and gallium-induced toxicity (Fig. 5). These results, coupled with previous results showing that $Ga(NTA)_2$ is able to compete for binding to hFbpA and form a stable complex (unpublished data), lead to the hypothesis that gallium may act as an iron analog and be bound and transported through hFbpABC. To test this, the iron transport assay was adapted for the use of radiolabeled gallium [$^{67}Ga(NTA)_2$]. Results show that the hFbpABC transporter functions in the direct uptake of gallium (Fig. 5D). Presumably, this transport gives rise to the gallium-induced toxicity which inhibits the growth of H-1443 *E. coli* expressing hFbpABC.

The hFbpA(Y196I)BC mutant transporter. We investigated the effect of a single-amino-acid mutation on hFbpABC transport activity through the construction and analysis of the hFbpA(Y195I)BC mutant transporter. This mutation, selected through assessment of the hFbpA crystal structure, targeted one of the conserved iron-liganding residues in the Fe^{3+} binding site of hFbpA (Fig. 6A). Alteration of this site is predicted to affect the ability of hFbpA to bind iron, as previously observed with a homologous nFbpA mutant. Using the radiolabeled iron transport assay, we assessed the impact of the hFbpA(Y196I) mutation on hFbpABC transport (Fig. 6B). The mutant exhibited ~35% activity of the hFbpABC wild-type transporter under standard conditions. The difference in activity was not due to altered expression levels of the binding proteins, as densitometric analysis demonstrated identical amounts of hFbpA and hFbpA(Y196I) (1:1.05, respectively). These results were unexpected in that one would expect the transport activity of the mutant to be completely lost, equating to that of the pBR322 vector-only control in this assay.

We hypothesized that the mutant protein had lost significant binding activity but retained diminished affinity for iron and thus might support lower levels of transport activity. To verify that hFbpA(Y196I) had indeed lost wild-type iron binding activity, the protein was purified and its iron binding characteristics were assessed. One of the signature characteristics that the iron binding proteins share with the transferrins is the presence of a strong visible absorption peak in the 480-nm range. This is attributable to hard ligand electron donors (phenolate tyrosines) that contribute to ligand-to-metal charge transfer upon interaction with Fe^{3+}. Comparison of visible spectra for wild-type hFbpA and mutant hFbpA(Y196I) demonstrated the complete loss of this peak from the mutant (Fig. 6C). Furthermore, trypsin susceptibility analysis of hFbpA(Y196I) resulted in no discernible Fe^{3+}-dependent resistance to trypsin proteolysis (data not shown), in similarity to a result previously observed in the nFbpA mutant (35). Equilibrium binding analysis of the mutant hFbpA(Y196I) protein demonstrated an iron dissociation constant in the submillimolar range ($K_d = 5.2 \times 10^{-4}$ M^{-1}) (Fig. 6D). This affinity is approximately 14 orders of magnitude weaker than the affinity of wild-type FbpA for Fe^{3+}. Substrate-dependent kinetic analysis, using conditions similar to those used with wild-type

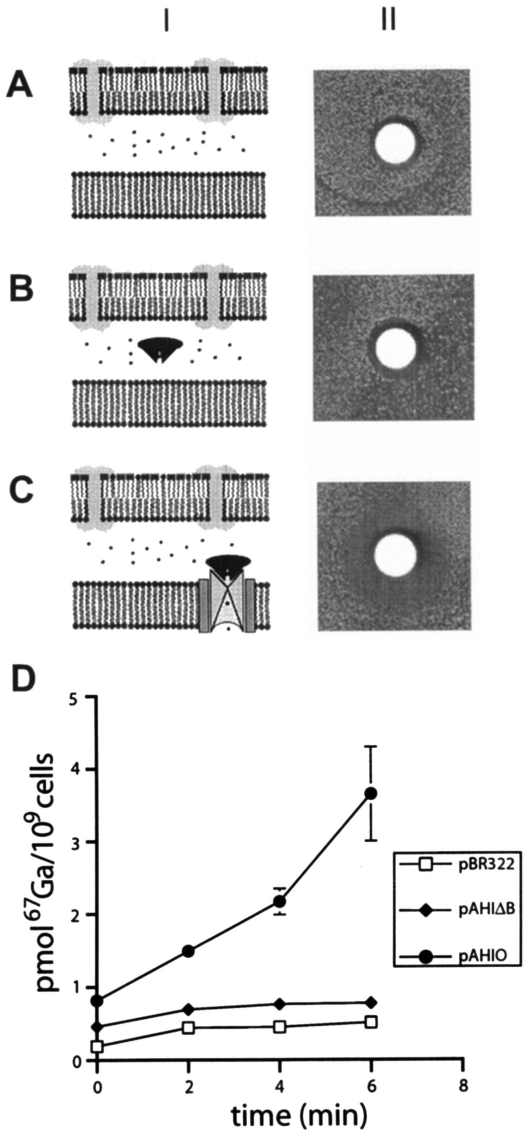

FIG. 5. hFbpABC-mediated gallium toxicity. (A) Sterile disks containing 10 μl 500 mM $Ga(NO_3)_3$ were applied to the plates. Following incubation, plates were digitally scanned. (A) H-1443/pBR322; (B) H-1443/pAHIΔB; (C) H-1443/pAHIO. (D) The $^{67}Ga(NTA)_2$ transport assay was conducted as described for $^{55}Fe(NTA)_2$ transport. Counts per minute for filters were determined using a gamma counter.

hFbpABC, demonstrated an estimated apparent K_m of 1.2 μM and an apparent V_{max} of 0.5 pmol/10^7cells/min. Although this K_m is similar to that of hFbpABC, the V_{max} is approximately one-third that of the wild-type transporter. Taken together, these data demonstrate that the hFbpA(Y196I) protein has lost significant iron binding activity, which correlates with a decrease in transport activity-capacity (V_{max}). However, this attenuated Fe^{3+} binding activity still supports a reduced level of transport, indicating that the mutant hFbpA(Y196I) protein is able to present the ABC transporter with Fe^{3+}. These results have interesting implications for the mechanism of hFbpABC-mediated transport in that it appears that high-affinity Fe^{3+} binding by hFbpA is not an absolute requisite for transport in this model system.

DISCUSSION

Expression of the *fbpABC* and *hitABC* operons in *E. coli* has provided important information regarding the biochemical basis of FbpABC transporter function. Several previous reports have noted the utility of a model system involving the siderophore-deficient *E. coli* H-1443 strain complemented with functional FbpABC loci from diverse pathogens, including *N. gonorrhoeae*, *S. marcescens*, and *H. influenzae* (1, 2, 6). We have employed this approach to investigate the biochemistry of hFbpABC transport in detail to gain information on the functional physiology of this novel transport system.

The results of this work support the function of hFbpABC as an ATP-dependent transporter with a high specificity for ferric iron. This is consistent with the fact that FbpA is known to bind metals in a manner analogous to that of transferrin and has a clear preference for ferric iron (11) (unpublished results). The fact that transferrin also binds other metals, including aluminum, gallium, copper, and zinc (43), is consistent with our observation that these metals compete for hFbpABC transport. FbpABC-mediated transport is a two-step process, the first step involving the binding of metal to FbpA and the second involving FbpA binding the FbpBC complex and metal transport into the cytosol. It is not clear whether these metals compete for transport at the level of competitive binding to hFbpA or whether they can indeed gain access to the cytosol and thus compete for cytoplasmic iron uptake. The exception to this is gallium. Metal sensitivity experiments (Fig. 5) demonstrate that while gallium may impart low-level toxicity to H-1443/pBR322 and H-1443/pAHIΔB cells (presumably through endogenous metal uptake systems), expression of a functional hFbpABC transporter causes an increased level of toxicity to H-1443/pAHIO. hFbpABC-mediated gallium transport is further demonstrated by the gallium transport assay (Fig. 5D). While gallium has an ionic radius (Ga^{3+}, 0.62 Å; Fe^{3+}, 0.65 Å) and a valence similar to those of ferric iron, it is not a transition metal and therefore cannot replace iron in the redox processes essential to many iron-containing proteins. Thus, the hFbpABC-mediated gallium-induced toxicity is likely the result of the entry of gallium into the cytosol and a general effect of cellular iron deprivation. Gallium toxicity has proven useful in subsequent functional studies of hFbpABC as a selection tool in the identification of hFbpABC mutants (unpublished data).

The hFbpA protein binds iron utilizing six coordinating ligands. This involves four protein side chains (His 9, Glu 57, Tyr 195, and Tyr 196) and two exogenous molecules, a synergistic anion and a water molecule, to complete the binding site (10). This repertoire of iron binding residues is highly conserved, as identical residues are employed by multiple FbpA homologs. Transferrin also utilizes a set of iron binding residues similar to FbpA, differing by only one side chain (glutamate is replaced with aspartate), consistent with the conservation of a highly specialized metal binding site. A functional result of this organization is the remarkable affinity for Fe^{3+} exhibited by both proteins.

In relation to the proposed hFbpA Fe^{3+} binding process (10), mutation of one of the tyrosine residues (Tyr 196 in hFbpA) would likely have a dramatic effect on Fe^{3+} binding, resulting in an altered affinity. Consistent with this, we have

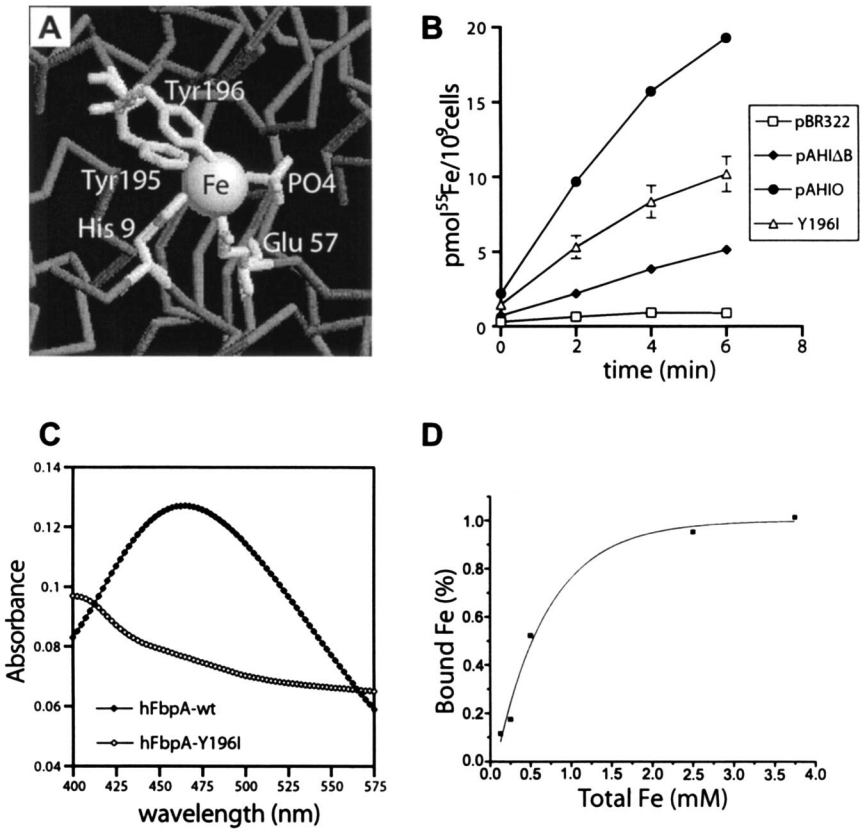

FIG. 6. The mutant hFbpA(Y196I)BC transporter. (A) View of the hFbpA metal binding site and Tyr196 targeted for mutation. (B) The hFbpA(Y196I)BC mutant transporter was tested via the radiolabeled iron transport assay and compared with pAHIO, pAHIΔB, and pBR322. The mutant demonstrates a rate of transport ~35% that of wild type. (C) Comparison of the characteristic 480-nm absorption peaks in the hFbpA wild-type and hFbpA(Y196I) mutant proteins. Loss of this peak correlates with a loss in high-affinity iron binding by hFbpA. (D) Equilibrium binding experiments verified the loss of high-affinity Fe^{3+} binding in hFbpA(Y196I). The protein has an effective dissociation constant (K_d) of 5.2 $\times 10^{-4}$ M^{-1} for $Fe(NTA)_2$, a drop in affinity of approximately 14 orders of magnitude compared with wild-type results.

measured a large decrease (~14 orders of magnitude) in the affinity of hFbpA(Y196I) for Fe^{3+} compared to that of wild type. Although this is a sizeable decrease, the new affinity value is in the overall range of affinities exhibited by PBPs from alternate binding protein-dependent ABC transport systems. This may account for the observation that the rate of iron transport is only moderately diminished (~35% of wild type) in this mutant transporter.

In other systems, it has been established that the second step of the transport process, binding of the PBP to the ABC transporter and substrate transport across the cytoplasmic membrane, is the rate-limiting step and that the affinity of the PBP for the substrate (K_d) roughly approximates the K_m of the transporter (36). Furthermore, mutant PBPs with decreased substrate binding affinities (K_d) do not necessarily correlate with a proportional decrease in transport (K_m) (48). These observations are likely explained by fact that the PBP is present at concentrations several orders of magnitude greater than the ABC transporter protein concentrations; PBP concentrations can reach the millimolar range within the periplasm (36). This is consistent with the results seen with the hFbpA(Y196I)BC transporter; the hFbpA(Y196I) protein with a K_d of ~500 μM gives rise to a transport rate ~35% that of the wild type. By extrapolation, it is plausible that an hFbpA mutant with a K_d of ~1 μM could support a rate of transport similar in scale to that of the wild type, although further investigations are required to verify this. If a binding protein with micromolar affinity is indeed sufficient for wild-type transport (in consistency with other systems), why then has FbpA evolved such a high natural Fe^{3+} binding affinity? This may have to do with several possible factors, including a role in (i) contributing to a thermodynamic driving force in the import of Fe^{3+} (from transferrin or lactoferrin), (ii) maintaining an available pool of Fe^{3+} within the periplasm for utilization in times of iron stress, or (iii) satisfying the requirements of maintaining ferric iron in a controlled protein environment to prevent reactivity-toxicity upon transit into the cell (16).

The FbpAs are novel PBPs in that they utilize a ternary anion in binding substrate (iron), they utilize a highly conserved set of iron binding residues, and they exhibit iron binding affinities 10 to 12 orders of magnitude greater than the affinities exhibited by typical PBPs for their respective substrates. These characteristics may be the result of the strict requirements that ferric iron places on proteins that must bind it, perhaps due to the propensity of free (naked) Fe^{3+} in aqueous, aerobic conditions to undergo hydrolysis and precipitate. The ability of ferric iron to induce cellular damage through hydroxyl-radical catalysis places additional constraints

on transport and management. Whether unique characteristics, based on the strict requirements of Fe^{3+} binding and transport, extend to the membrane permease and ATP binding protein components of the FbpABC transporters is an area of present study.

Although FbpABC is the first identified ferric Fe^{3+}-specific ABC transporter, several alternate systems that have free-iron transport activity, including the ferrous iron transport system *feoABC*, specific for ferrous iron under anaerobic conditions, and the CorA magnesium transport system, transporting Fe^{2+} with low affinity under low-magnesium conditions, have been identified (24, 25). Both these systems require free iron in the reduced soluble form, Fe^{2+}. An additional metal transporter, MntH, is a bacterial homolog of the NRAMP (natural resistance against microbial pathogens) family of eukaryotic metal permeases (12, 28) and demonstrates specificity towards manganese and lower selectivity towards ferrous iron, zinc, and other metals. However, it functions as an individual permease independent of a binding protein and is energized through protonmotive force. Recently, a stimulator of Fe transport system has been identified, with homologs thus far identified in humans (23) and yeast (*S. cerevisiae*) (42) and a putative stimulator of Fe transport system identified in bacteria (*B. subtilis*) (42). Although the function of these transporters remains largely undescribed, they appear to be specific for ferric iron. Generally speaking, these systems appear to be driven by individual membrane permeases that function in both ATP hydrolysis and metal transport without the interplay of a separate PBP and ATP binding protein. Additionally, they may require the presence of both an iron oxidase and reductase for function. Further detailed investigations of the FbpB and FbpC proteins are required for fuller understanding of the novel structural and functional aspects of ferric iron-specific FbpABC transport.

In conclusion, the FbpABC iron transporters have several characteristics common to the family of bacterial binding protein-dependent ABC transporters, including similar kinetics and the use of ATP hydrolysis as the energy source driving transport. The transporters are highly selective for Fe^{3+} and have a preference for trivalent metals, including Ga^{3+}. Interestingly, the transporters possess characteristics which may be shared by other iron transport systems and may have additional attributes specifically related to the transport of free ferric iron. Homologs of FbpABC and individual components thereof have recently been identified in numerous bacteria, including *Yersinia* spp. (21), *Campylobacter jejuni* (20), *Pasteurella haemolytica* (27), and *Actinobacillus actinomycetemcomitans* (46); ongoing genome projects will undoubtedly uncover further homologs. Therefore, the FbpABC transporters may comprise a widely employed iron acquisition system with implications for virulence among many diverse bacterial species.

ACKNOWLEDGMENTS

We thank K.G. Vaughan, C. B. Bahr, and S. M. Phadke for technical and editorial assistance.

This work was supported by National Institutes of Health grant R29 A132226 (T.A.M.).

REFERENCES

1. **Adhikari, P., S. A. Berish, A. J. Nowalk, K. L. Veraldi, S. A. Morse, and T. A. Mietzner.** 1996. The *fbpABC* locus of *Neisseria gonorrhoeae* functions in the periplasm-to-cytosol transport of iron. J. Bacteriol. **178:**2145–2149.
2. **Adhikari, P., S. D. Kirby, A. J. Nowalk, K. L. Veraldi, A. B. Schryvers, and T. A. Mietzner.** 1995. Biochemical characterization of a *Haemophilus influenzae* periplasmic iron transport operon. J. Biol. Chem. **270:**25142–25149.
3. **Alexeev, D., H. Zhu, M. Guo, W. Zhong, D. J. Hunter, W. Yang, D. J. Campopiano, and P. J. Sadler.** 2003. A novel protein-mineral interface. Nat. Struct. Biol. **10:**297–302.
4. **Ames, G. F. L., C. E. Liu, A. K. Joshi, and K. Nikaido.** 1996. Liganded and unliganded receptors interact with equal affinity with the membrane complex of periplasmic permeases, a subfamily of traffic ATPases. J. Biol. Chem. **271:**14264–14270.
5. **Angerer, A., S. Gaisser, and V. Braun.** 1990. Nucleotide sequences of the *sfuA*, *sfuB*, and *sfuC* genes of *Serratia marcescens* suggest a periplasmic-binding-protein-dependent iron transport mechanism. J. Bacteriol. **172:**572–578.
6. **Angerer, A., B. Klupp, and V. Braun.** 1992. Iron transport systems of *Serratia marcescens*. J. Bacteriol. **174:**1378–1387.
7. **Bagg, A., and J. B. Neilands.** 1987. Ferric uptake regulation protein acts as a repressor, employing iron (II) as a cofactor to bind the operator of an iron transport operon in *Escherichia coli*. Biochemistry **26:**5471–5477.
8. **Boukhalfa, H., D. S. Anderson, T. A. Mietzner, and A. L. Crumbliss.** 2003. Kinetics and mechanism of iron release from the bacterial ferric binding protein nFbp: exogenous anion influence and comparison with mammalian transferrin. J. Biol. Inorg. Chem. **8:**881–892.
9. **Braun, V., R. Gross, W. Koster, and L. Zimmermann.** 1983. Plasmid and chromosomal mutants in the iron(III)-aerobactin transport system of *Escherichia coli.* Use of streptonigrin for selection. Mol. Gen. Genet. **192:**131–139.
10. **Bruns, C. M., D. S. Anderson, K. G. Vaughan, P. A. Williams, A. J. Nowalk, D. E. McRee, and T. A. Mietzner.** 2001. Crystallographic and biochemical analyses of the metal-free *Haemophilus influenzae* Fe^{3+}-binding protein. Biochemistry **40:**15631–15637.
11. **Bruns, C. M., A. J. Nowalk, A. S. Arvai, M. A. McTigue, K. G. Vaughan, T. A. Mietzner, and D. E. McRee.** 1997. Structure of *Haemophilus influenzae* $Fe(^{+3})$-binding protein reveals convergent evolution within a superfamily. Nat. Struct. Biol. **4:**919–924.
12. **Cellier, M., G. Prive, A. Belouchi, T. Kwan, V. Rodrigues, W. Chia, and P. Gros.** 1995. Nramp defines a family of membrane proteins. Proc. Natl. Acad. Sci. USA **92:**10089–10093.
13. **Chen, C. Y., S. A. Berish, S. A. Morse, and T. A. Mietzner.** 1993. The ferric iron-binding protein of pathogenic *Neisseria* spp. functions as a periplasmic transport protein in iron acquisition from human transferrin. Mol. Microbiol. **10:**311–318.
14. **Crosa, J.** 1989. Genetics and molecular biology of siderophore-mediated iron transport in bacteria. Microbiol. Rev. **53:**517–530.
15. **De Lorenzo, V., M. Herrero, F. Giovannini, and J. B. Neilands.** 1988. Fur (ferric uptake regulation) protein and CAP (catabolite-activator protein) modulate transcription of fur gene in *Escherichia coli*. Eur. J. Biochem. **173:**537–546.
16. **Dhungana, S., C. H. Taboy, D. S. Anderson, K. G. Vaughan, P. Aisen, T. A. Mietzner, and A. L. Crumbliss.** 2003. The influence of the synergistic anion on iron chelation by ferric binding protein, a bacterial transferrin. Proc. Natl. Acad. Sci. USA **100:**3659–3664.
17. **Fecker, L., and V. Braun.** 1983. Cloning and expression of the *fhu* genes involved in iron(III)-hydroxamate uptake by *Escherichia coli*. J. Bacteriol. **156:**1301–1314.
18. **Ferenci, T., M. Muir, K. S. Lee, and D. Maris.** 1986. Substrate specificity of the *Escherichia coli* maltodextrin transport system and its component proteins. Biochim. Biophys. Acta **860:**44–50.
19. **Gabricevic, M., D. S. Anderson, T. A. Mietzner, and A. L. Crumbliss.** 2004. Kinetics and mechanism of iron(III) complexation by ferric binding protein: the role of phosphate. Biochemistry **43:**5811–5819.
20. **Galindo, M. A., W. A. Day, B. H. Raphael, and L. A. Joens.** 2001. Cloning and characterization of a *Campylobacter jejuni* iron-uptake operon. Curr. Microbiol. **42:**139–143.
21. **Gong, S., S. W. Bearden, V. A. Geoffroy, J. D. Fetherston, and R. D. Perry.** 2001. Characterization of the *Yersinia pestis* Yfu ABC inorganic iron transport system. Infect. Immun. **69:**2829–2837.
22. **Guo, M., I. Harvey, W. Yang, L. Coghill, D. J. Campopiano, J. A. Parkinson, R. T. MacGillivray, W. R. Harris, and P. J. Sadler.** 2003. Synergistic anion and metal binding to the ferric ion-binding protein from *Neisseria gonorrhoeae*. J. Biol. Chem. **278:**2490–2502.
23. **Gutierrez, J. A., J. Yu, S. Rivera, and M. Wessling-Resnick.** 1997. Functional expression cloning and characterization of SFT, a stimulator of Fe transport. J. Cell Biol. **139:**895–905. (Erratum, **147:**204, 1999.)
24. **Hantke, K.** 1997. Ferrous iron uptake by a magnesium transport system is toxic for *Escherichia coli* and *Salmonella typhimurium*. J. Bacteriol. **179:**6201–6204.
25. **Kammler, M., C. Schon, and K. Hantke.** 1993. Characterization of the ferrous iron uptake system of *Escherichia coli*. J. Bacteriol. **175:**6212–6219.
26. **Khun, H. H., V. Deved, H. Wong, and B. C. Lee.** 2000. *fbpABC* gene cluster in *Neisseria meningitidis* is transcribed as an operon. Infect. Immun. **68:**7166–7171.

27. **Kirby, S. D., F. A. Lainson, W. Donachie, A. Okabe, M. Tokuda, O. Hatase, and A. B. Schryvers.** 1998. The *Pasteurella haemolytica* 35 kDa iron-regulated protein is an FbpA homologue. Microbiology **144:**3425–3436.
28. **Makui, H., E. Roig, S. T. Cole, J. D. Helmann, P. Gros, and M. F. Cellier.** 2000. Identification of the *Escherichia coli* K-12 Nramp orthologue (MntH) as a selective divalent metal ion transporter. Mol. Microbiol. **35:**1065–1078.
29. **Manson, M. D., W. Boos, P. J. Bassford, Jr., and B. A. Rasmussen.** 1985. Dependence of maltose transport and chemotaxis on the amount of maltose-binding protein. J. Biol. Chem. **260:**9727–9733.
30. **Mietzner, T. A., and S. A. Morse.** 1994. The role of iron-binding proteins in the survival of pathogenic bacteria. Annu. Rev. Nutr. **14:**471–493.
31. **Mietzner, T. A., S. B. Tencza, K. G. Vaughan, P. A. Adhikari, and A. J. Nowalk.** 1998. Periplasm-to-cytosol free Fe(III) transporters of pathogenic gram-negative bacteria. Curr. Top. Microbiol. Immunol. **225:**113–135.
32. **Neilands, J. B.** 1984. Methodology of siderophores. Struct. Bonding **58:**1–24.
33. **Neilands, J. B.** 1980. Microbial metabolism of iron, p. 529–572. *In* A. Jacobs and M. Worwood (ed.), Iron in biochemistry and medicine, vol. 2. Academic Press, Inc., New York, N.Y.
34. **Nowalk, A., S. Tencza, and T. Mietzner.** 1994. Coordination of iron by the ferric-iron binding protein of pathogenic *Neisseria* is homologous to the transferrins. Biochemistry **33:**12769–12775.
35. **Nowalk, A. J., K. J. Vaughan, B. Day, S. B. Tencza, and T. A. Mietzner.** 1997. Metal-dependent conformers of the periplasmic ferric ion binding protein. Biochemistry **36:**13054–13059.
36. **Prossnitz, E., A. Gee, and G. F. Ames.** 1989. Reconstitution of the histidine periplasmic transport system in membrane vesicles. Energy coupling and interaction between the binding protein and the membrane complex. J. Biol. Chem. **264:**5006–5014.
37. **Schryvers, A. B., and I. Stojiljkovic.** 1999. Iron acquisition systems in the pathogenic *Neisseria*. Mol. Microbiol. **32:**1117–1123.
38. **Shouldice, S. R., D. R. Dougan, R. J. Skene, L. W. Tari, D. E. McRee, R. H. Yu, and A. B. Schryvers.** 2003. High resolution structure of an alternate form of the ferric ion binding protein from *Haemophilus influenzae*. J. Biol. Chem. **278:**11513–11519.
39. **Shouldice, S. R., D. R. Dougan, P. A. Williams, R. J. Skene, G. Snell, D. Scheibe, S. Kirby, D. J. Hosfield, D. E. McRee, A. B. Schryvers, and L. W. Tari.** 2003. Crystal structure of *Pasteurella haemolytica* ferric ion-binding protein A reveals a novel class of bacterial iron-binding proteins. J. Biol. Chem. **278:**41093–41098.
40. **Shouldice, S. R., R. J. Skene, D. R. Dougan, D. E. McRee, L. W. Tari, and A. B. Schryvers.** 2003. Presence of ferric hydroxide clusters in mutants of *Haemophilus influenzae* ferric ion-binding protein A. Biochemistry **42:**11908–11914.
41. **Staudenmaier, H., B. Van Hove, Z. Yaraghi, and V. Braun.** 1989. Nucleotide sequences of the *fecBCDE* genes and location of the proteins suggest a periplasmic-binding protein-dependent transport mechanism for iron(III) dicitrate in *Escherichia coli*. J. Bacteriol. **171:**2626–2633.
42. **Stearman, R., D. S. Yuan, Y. Yamaguchi-Iwai, R. D. Klausner, and A. Dancis.** 1996. A permease-oxidase complex involved in high-affinity iron uptake in yeast. Science **271:**1552–1557.
43. **Sun, H., M. C. Cox, H. Li, A. B. Mason, R. C. Woodworth, and P. J. Sadler.** 1998. [1H,13C] NMR determination of the order of lobe loading of human transferrin with iron: comparison with other metal ions. FEBS Lett. **422:** 315–320.
44. **Taboy, C. H., K. G. Vaughan, T. A. Mietzner, P. Aisen, and A. L. Crumbliss.** 2001. Fe^{3+} coordination and redox properties of a bacterial transferrin. J. Biol. Chem. **276:**2719–2724.
45. **Weinberg, E. D.** 1984. Iron withholding: a defense against infection and neoplasia. Physiol. Rev. **64:**65–102.
46. **Willemsen, P. T., I. Vulto, M. Boxem, and J. de Graaff.** 1997. Characterization of a periplasmic protein involved in iron utilization of *Actinobacillus actinomycetemcomitans*. J. Bacteriol. **179:**4949–4952.
47. **Winkelmann, F., D. van der Helm, and J. B. Neilands (ed.).** 1987. Iron transport in microbes, plants and animals. VCH, Weinheim, Germany.
48. **Wolf, A., E. W. Shaw, K. Nikaido, and G. F. Ames.** 1994. The histidine-binding protein undergoes conformational changes in the absence of ligand as analyzed with conformation-specific monoclonal antibodies. J. Biol. Chem. **269:**23051–23058.
49. **Zak, O., A. Leibman, and P. Aisen.** 1983. Metal-binding properties of a single-sited transferrin fragment. Biochim. Biophys. Acta **742:**490–495.
50. **Zhu, H., D. Alexeev, D. J. Hunter, D. J. Campopiano, and P. J. Sadler.** 2003. Oxo-iron clusters in a bacterial iron-trafficking protein: new roles for a conserved motif. Biochem. J. **376:**35–41.